Machine Learning Models for Analyzing FBG Pressure Sensor Data in Monitoring Leak in Water Pipeline

Hossam Youssef, Matthias Fabian, Mounib Khanafer, *Senior Member, IEEE*, Sumsun Naher, Kenneth TV Grattan, and Tong Sun

***Abstract*— Aging water and sewage pipelines require effective monitoring as leakage and burst incidents pose environmental, economic, and public safety risks. Many existing studies rely on laboratory or simulated data from electrical sensors installed in harsh sewer environments, which require regular cleaning and calibration. The novelty of this work lies in presenting a systematic, real-world evaluation of machine learning models for pipeline leak detection using fiber Bragg grating-based pressure sensors deployed in an operational pipeline test facility for the first time. The models evaluated include supervised models, such as Random Forest and Extreme Gradient Boosting (XGBoost), and unsupervised models, such as Long Short-Term Memory (LSTM) and LSTM Autoencoder. These models are compared under identical experimental conditions and were evaluated under both serial (single sensor) and parallel (multi-sensor) configurations, using sliding windows of varying lengths. Weighted precision and F1-scores were used to address strong class imbalance across leak sizes. Results show that XGBoost achieved the best overall performance, reaching 77% precision and 52% F1-score at a 45-point window length. The results obtained are better than those reported in previous work, most of which rely on simulations or laboratory datasets and critically do not evaluate models under real operational pipeline conditions, as is done here. The findings demonstrate the robustness of supervised XGBoost when applied to small, noisy real-world datasets and they highlight the feasibility of integrating ML-based FBG sensors into cloud-enabled pipeline monitoring systems.**

***Index Terms*—Fiber Bragg grating (FBG) sensor, leak detection, machine learning, pipeline monitoring.**

I. INTRODUCTION

THE aging water and sewage pipelines pose significant environmental, economic, and public safety risks. Rising leak and burst incidents, such as those reported in Gloucester (May 2025) and Oxford (July 2025) [1], [2], highlight the need for reliable real-time leak detection systems capable of continuous operation in harsh environments.

Fiber Bragg grating (FBG) pressure sensors have emerged as promising candidates for pipeline monitoring applications due to their immunity to electromagnetic interference, corrosion resistance, and high sensitivity [3]-[5]. FBG-based sensors have been used to characterize pipeline flow and leaks via physics-based signal analysis [6]-[9]. For example, Bian et al. have estimated flow velocity using flow-induced vibration, without using Machine Learning (ML) [9]. However, these methods depend on manual feature engineering and calibration, limiting robustness under varying conditions. ML instead learns nonlinear patterns directly from raw data, enhancing adaptability, scalability, and real-time leak detection without explicit physical modeling. An example of this is in the work of Jia et al. who combined FBG hoop strain sensors with a BP neural network for leak localization under simulated transient conditions [10]. Thus, while prior work has demonstrated the feasibility (and indeed value) of FBG-based leak detection [11], no reported study has systematically compared supervised and unsupervised ML models using real-time FBG pressure data from an operational test facility. Existing ML approaches often rely on electronic or acoustic sensors and offline or laboratory datasets, lacking structured comparisons under varying leak conditions [10], [12]. This work distinguishes itself by using a dataset collected from the National Distributed Water Infrastructure Facility at the University of Sheffield in the UK, in which the system was subjected to various leak conditions.

Further, ML has been widely applied to leak detection using electrical and acoustic sensors in laboratory or simulated environments, often reporting a very satisfactory performance [13]-[27]. However, models developed, and which are based solely on simulated data may not generalize to real-world conditions, where environmental variability, noise, and class imbalance are inherent. Several IoT-based studies have been reported which combine ML with electronic or acoustic sensors. For example, João et al. [13] achieved 85% accuracy in laboratory settings and 75% in field trials using a wireless flow sensor network with Random Forest. Large-scale deployments such as the Dubai Electricity and Water Authority (DEWA) system reported 66–85% precision using electronic flow, pressure, and temperature sensors with ML models including Isolation Forest, SVM, and LSTM [14]. Deep learning approaches, such as 1D-CNN for acoustic sensing [15] and

This work was supported by City St George's, University of London for providing the scholarship for PhD study. (Corresponding author: Hossam Youssef.) H. Youssef, M. Fabian, S. Naher, K. T. V. Grattan, and T. Sun are with the School of Science and Technology, City St George's, University of London, London, United Kingdom (e-mail: hossam.youssef@city.ac.uk; matthias.fabian.1@city.ac.uk; sumsun.naher.1@city.ac.uk; K.T.V.Grattan@city.ac.uk; t.sun@city.ac.uk).

M. Khanafer is with College of Engineering and Applied Sciences, American University of Kuwait, Kuwait (e-mail: mkhanafer@auk.edu.kw).

embedded ML on low-power devices [16], have also been explored. Despite promising results, these systems rely on power-driven electronics susceptible to energy constraints, degradation, and calibration drift in harsh sewer environments. By contrast, FBG-based sensors offer durability, a multiplexing capability, and thus good suitability for corrosive conditions [4]. Yang et al. [28] achieved 97% accuracy in oil and gas pipelines using FBG-based vibration and acoustic sensing with CNN-Bi LSTM, while Gemeinhardt et al. [29] have reported an F1-score of 90% using distributed temperature and acoustic sensing in laboratory experiments. Additional studies investigated FBG-based pipeline protection and multi-leak classification [30]-[37]. However, most existing work remains limited to controlled or simulated conditions and does not provide the important systematic comparisons of supervised and unsupervised ML models using real-world FBG-based pressure data from operational test facilities.

The most relevant studies are summarized in Table I, highlighting sensor types, environments, models, and reported performance. As shown, the majority rely on simulated or controlled datasets from electronic or distributed acoustic sensors.

TABLE I
Machine learning leak detection studies

Study	Sensor Type	Environment	Model	Metric
João et al. [13]	Flow Sensors	Lab +Field	RF	85% accuracy
DEWA [14]	Pressure, Temperature Sensors	Real	SVM	85% Precision
Islam et al. [16]	Microphone (acoustic)	Lab	ANN	98% accuracy
Zang et al. [21]	pressure sensor	Simulated Data	SVM	98% accuracy
Yang et al. [28]	FBG sensors (acoustic)	Lab	CNN + Bi LSTM	97% accuracy
Gemeinhardt et al. [29]	FBG sensors (acoustic)	Lab	DFM	90% F1 score

To the best of the authors' knowledge, no prior study has systematically compared supervised and unsupervised ML algorithms using real-world FBG pressure data from a pipeline test facility. This paper evaluates both learning paradigms under serial and parallel sensor configurations and benchmarks their performance against state-of-the-art leak detection models reported in the literature.

II. DATASET AND PREPROCESSING

In this study, data were collected from four surface-mounted FBG-based pressure sensors (S1–S4) installed on a 37 m high-density polyethylene pipeline at the National Distributed Water Infrastructure Facility, University of Sheffield, UK (see Fig. 1). As shown in Fig.1 (a), water was supplied by a constant 5m header tank (0.5 bar) with a U-bend section near the end ensuring that the pipe is always full, i.e. providing reliable pressure readings. A leak inducing valve was positioned centrally between them to generate pressure transients which then propagated along the pipeline. Variations in the sensor-to-leak distance resulted in different signal magnitudes, directly influencing the wavelength responses used for ML analysis. Fig.1 (b) shows a sensor attached securely to the pipe to ensure effective pressure transfer. Fig.1 (c) shows the leak size was adjusted by changing disks, each with different hole sizes. Further information on the detailed sensor design and installation issues, which are beyond the scope of this paper, are reported in for example the work of Venketeswaran et al. [37].

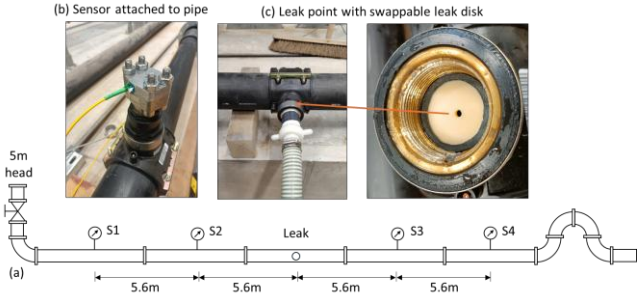

Fig. 1. Full pipeline layout at the National Distributed Water Infrastructure Facility, University of Sheffield, UK. (a) Experiment layout; (b) Sensor attached to pipe; (c) Leak point.

Fig. 2 shows representative sensor responses to a 12 mm leak test schedule. Each test started with a zero-pressure baseline which was recorded for approximately 150 s. The main valve (Fig. 1(a)) was then opened, and the flow was allowed to stabilize for 120 s, before the leak valve was opened for around 60 s. This was followed by stable flow for 90 s, before the main valve was closed. This was repeated 20 times for different leak sizes with inherent class imbalance (see data in Table II).

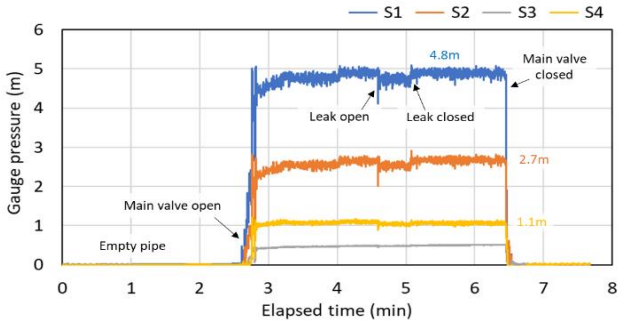

Fig. 2. Representative experimental leak test showing gauge pressure at four different sensor locations (S1–S4).

Data were acquired using an FBG interrogator (Micron Optics si155), with raw wavelength signals recorded at 5 kHz. For ML processing, signals were down-sampled to 17 Hz after evaluating multiple rates, as this preserved leak dynamics while reducing computational and bandwidth requirements.

Fig. 3 shows a spectrogram of the leak event (±10 s). The Nyquist frequency (8.5 Hz) of the 17 Hz down-sampled signal

was marked by the white line. The dominant leak energy was seen to lie below this limit, indicating that down-sampling does not remove the critical frequency components.

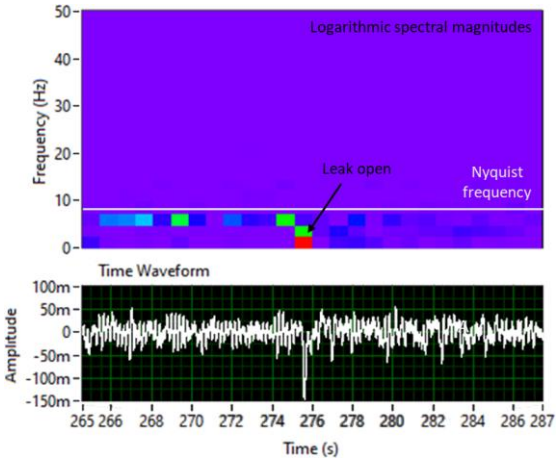

Fig. 3. Spectrogram of leak event showing dominant energy below the Nyquist frequency (8.5 Hz) of the 17 Hz down-sampled signal.

TABLE II
Dataset distribution by leak size

Leak size (mm)	Number of test files
12	3
10	7
8	6
7	4

III. Machine Learning Models and Evaluation Protocol

A. Model Overview

Both supervised and unsupervised models were evaluated to provide a balanced comparison across learning paradigms for 'true-to-life' noisy FBG time-series data. Random Forest (RF) and Extreme Gradient Boosting (XGBoost) were selected as supervised baselines due to their robustness to noise, nonlinear modeling capability, and strong performance on small, imbalanced datasets, with RF reducing variance via ensemble averaging and XGBoost using regularized gradient-boosted trees for improved generalization [39], [40]. Long Short-Term Memory (LSTM) and LSTM Autoencoder (LSTM-AE) were included to capture temporal dependencies [41], [42]. RF and XGBoost were trained on labeled 'leak/no-leak' data, while LSTM and LSTM-AE were trained only on 'no-leak' samples, with anomalies identified via prediction or reconstruction thresholds. This setup enables a systematic comparison between tree-based ensembles and deep recurrent architectures, under identical experimental conditions.

B. Training and Testing Procedure

To ensure reproducibility and avoid temporal bias, the dataset was split by file into 70% training, 15% validation, and 15% testing using a fixed random seed (42). This prevented data from the same file appearing in multiple sets. The models were evaluated under two input configurations:

a) Serial mode: Single input with all sensor data treated as a 1D sequence (Fig. 4 Top).
b) Parallel mode: Individual inputs for each sensor, capturing cross-sensor correlations (Fig. 4 Bottom).

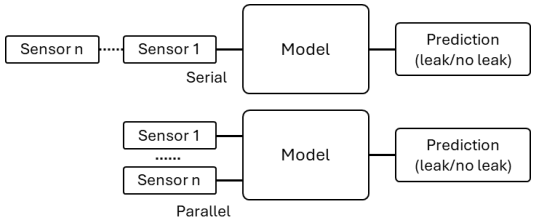

Fig. 4. Input configurations: (Top) Serial mode, single sensor input; (Bottom) Parallel mode, multi sensors input (n=4).

Overlapping sliding windows of size $W \in \{1, 5, 10, 15, \ldots, 50\}$ with step size of 1 were applied to 17 Hz down-sampled signals (0.06–2.94 s spans). As leak onsets occur over 1 s (Fig. 2), this range captures transients and early steady-state behavior, while limiting detection latency. The window length was capped at 50 samples to satisfy real-time constraints. Signals were z-score normalized using training data. Models were implemented in Python (Scikit-learn, TensorFlow/Keras).

In a parallel configuration, models assumed all sensor channels are available. In practice, however, dropouts can and will occur due to communication loss or hardware faults. During preprocessing, missing or faulty samples can be identified using not a number (NaN), out-of-range, and flatline checks, and the affected windows are flagged. If a fault was detected, parallel inference would be suspended and a data-quality alarm then issued until valid multichannel data operation resumes, preventing unreliable predictions and explicitly notifying operators.

C. Hyperparameter Settings

To maintain a fair comparison and to emphasize architectural differences rather than parameter tuning, hyperparameters were fixed across all experiments rather than optimized, as shown:

- RF: 200 trees (serial) / 300 trees (parallel), max depth = 10
- XGBoost: 300 estimators, max depth = 6, learning rate = 0.05
- LSTM: 1–2 layers (32–64 units), 50 epochs, batch size = 128
- Encoder-decoder 64-32-32-64 architecture, 50 epochs, batch size = 128

These parameters are chosen to balance model complexity and computational efficiency while isolating structural differences between supervised and unsupervised learning approaches.

D. Evaluation Metrics

Leak detection was formulated as a binary classification (leak = 1, no-leak = 0). Given the strong class imbalance, accuracy was not used; instead, the following metrics were computed:

- Precision: proportion of correctly identified leaks among all predicted leaks, emphasizing low false-positive rates.
- Recall: proportion of actual leaks correctly identified.
- F1-score: balancing precision and recall.

To address the imbalance in leak sizes (different numbers of datasets for each leak size), weighted averages were computed using both the number of datasets N_i and leak size i. To reflect that smaller leaks are harder to detect, a difficulty factor d_i was defined as inversely proportional to the leak size as $d_i = \frac{1}{i}$. The weight w_i assigned to each leak size category was then computed as [43]-[46]:

$$w_i = \frac{N_i d_i}{\sum(N_i d_i)} \quad (1)$$

Where:

- w_i is the normalized weight for leak size i.
- N_i is the number of test files available for leak size i.
- d_i is the inverse of leak size.

Table III lists the resulting weights used for calculating the average. The weighted average of a metric M (e.g., precision or recall) was computed as:

$$Weighted\ Metric\ Average = \sum w_i\, M_i \quad (2)$$

Additionally, the Signal-to-Noise Ratio (SNR) between leak and no-leak intervals was calculated to quantify leak detectability as follows [47], [48]:

$$SNR = \frac{\mu_{no\_leak} - min\ (leak)}{\sigma_{no\_leak}} \quad (3)$$

Where μ_{no_leak} and σ_{no_leak} are the mean and standard deviation of the baseline (no-leak) interval, and min (leak) is the minimum signal magnitude of a leak event. The larger the leak size, the larger the drop in the signal, as shown in Fig. 6 for leaks sizes of 7 mm and 12 mm. Despite some leak-induced wavelength changes being comparable to background noise (Fig. 5), good detection has been achieved by exploiting sliding windows and multiple sensor signals inputs to capture temporal patterns and cross-sensor correlations, enabling robust performance even under low SNR. This highlights the role of temporal context and sensor fusion in practical pipeline monitoring.

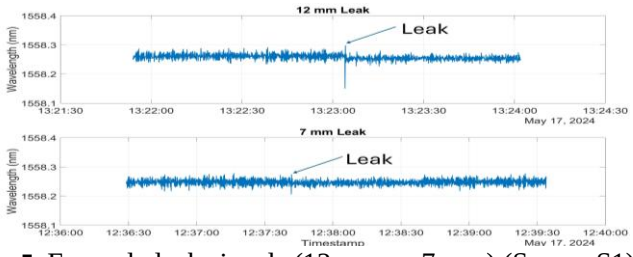

Fig. 5. Example leak signals (12 mm vs 7 mm) (Sensor S1). Larger leaks yield larger deviations.

Equation (3) measures leak deviation from baseline noise, with higher SNR indicating easier detectability. SNR was computed across all sensors and files and averaged by leak size. Fig. 6 confirms that larger leaks yield higher SNR values.

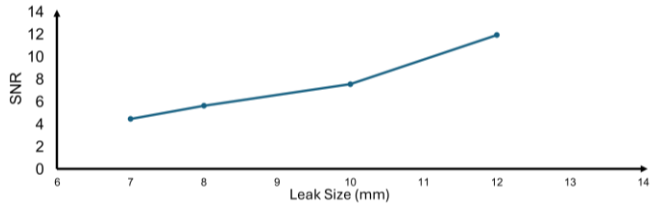

Fig. 6. Average SNR vs leak size confirming higher detectability for large leaks.

TABLE III
Weights used for weighted averages.

Leak Size i (mm)	Number of test files N_i	Weight of leak size $1/d_i$
12	3	1/12
10	7	1/10
8	6	1/8
7	4	1/7

IV. Results and Discussion

All models were evaluated under serial and parallel configurations across varying window sizes, revealing clear effects of data fusion and temporal context on precision and detection reliability.

A. Precision

Fig. 7 shows serial-configuration precision results. All models performed similarly below 50% for small windows, while LSTM and LSTM Autoencoder improved at window size 20 and beyond. Nevertheless, no model surpassed 55% precision, highlighting the limited capability of single-sensor analysis.

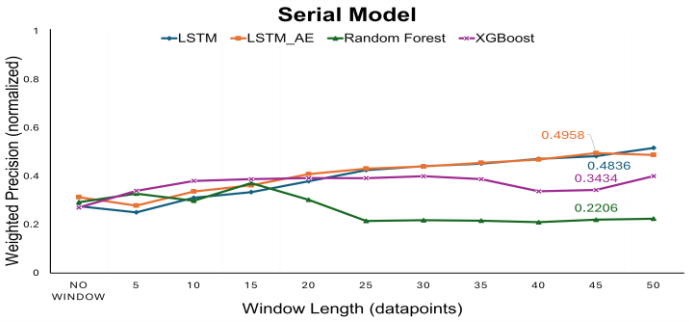

Fig. 7. Precision (serial mode) vs window length for all models. Windowing improves LSTM, but precision remains <50%.

In contrast, parallel configuration (Fig. 8) significantly improved performance, with XGBoost reaching 77.4% precision at a 45-sample window. Multi-sensor fusion

enhanced contextual learning, while no additional improvement was observed beyond 50 samples.

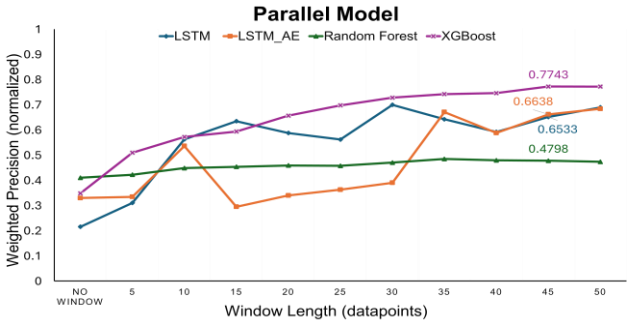

Fig. 8. Precision (parallel mode) vs. window size. XGBoost peaks at 77.4% for W = 45.

B. Recall

Recall for serial and parallel modes is shown in Figs. 9 and 10, respectively. In both configurations, tree-based models generally achieved higher recall than sequence-based deep models, but at the expense of increased false positives and reduced precision. Transitioning from serial to parallel mode slightly decreased recall while improving precision, indicating a tighter decision boundary with multiple sensor input. Overall, window length affected the recall less than the precision.

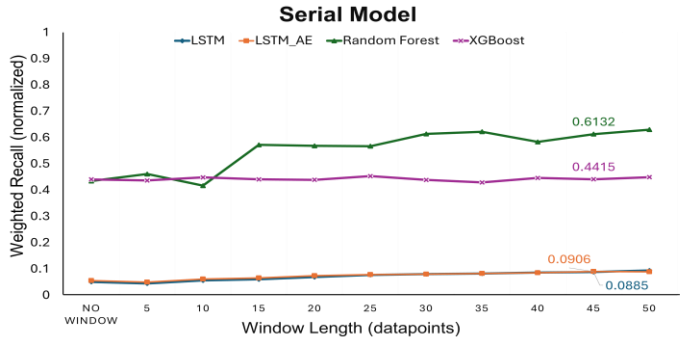

Fig. 9. Recall (serial mode) vs. window size. Tree-based models show higher recall.

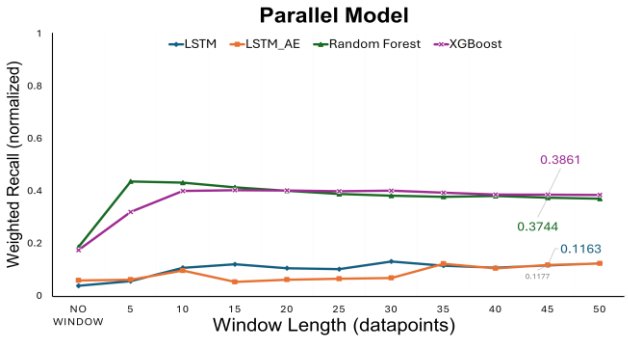

Fig. 10. Recall (parallel mode) vs. window size. Slight recall drop accompanies precision gain.

C. F1-Score

Fig. 11 presents the F1-scores for all models. In serial mode, models remained below 50%, whereas XGBoost reached approximately 52% in parallel mode (W = 45). These results indicate that moderate temporal context provides optimal performance by preserving short-term transients without over-smoothing.

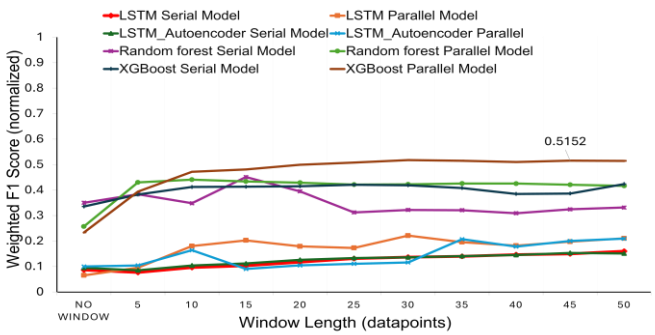

Fig. 11. F1-score vs. window size. XGBoost attains the best balance around W = 30–45.

D. Confusion Matrix

The confusion matrix for XGBoost in parallel mode (W = 45) (Fig. 12) shows consistent detection of leaks ≥ 7 mm with limited false alarms. Most false positives occurred near leak start and end boundaries, where gradual pressure transitions made ground-truth labeling uncertain.

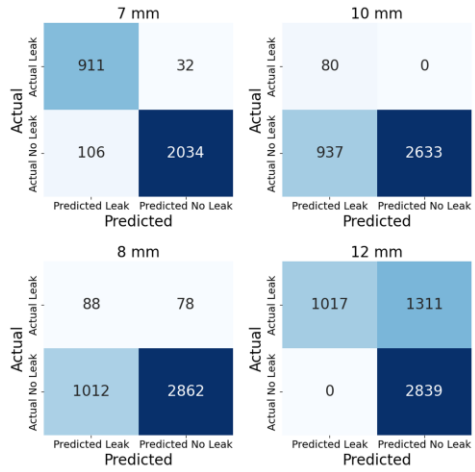

Fig. 12. Confusion matrices for XGBoost (W = 45).

E. Key findings

Several key insights can be seen to emerge from these results:

1. Parallel training outperformed serial training, demonstrating the advantage of multiple sensor input. Serial training is still viable for single-sensor deployments but requires balanced data for robustness. Unsupervised LSTMs can achieve high precision with sufficiently large and balanced datasets.
2. XGBoost achieved the highest precision and F1-score, outperforming other models and demonstrating its suitability for small, imbalanced real-world datasets.
3. Longer windows improved precision and F1 by capturing temporal context, with 30–45 points offering the best trade-off between context and fragmentation.

4. Precision is crucial in pipeline monitoring to avoid costly false alarms; achieving 77.4% weighted precision supports real-world deployment feasibility.
5. Limited real-world leak data (≥7 mm events only) constrained generalization; broader datasets with smaller leaks and varying pressures are needed to improve recall and transferability.
6. In practical deployments, underground access may limit the number of sensors that can be used. Based on the testbed layout (Fig. 1(a)), placing two sensors around high-risk segments improves leak detectability by capturing local pressure changes and cross-sensor consistency. In situations where only one sensor is available, placement should prioritize leak locations (e.g., joints, valves, service connections, bends, and diameter transitions) and be as close as possible to the monitored segment. While this study uses a fixed laboratory layout, ongoing wastewater trials are planned to validate these strategies under real access constraints and inform evidence-based placement guidelines.
7. Cloud-enabled monitoring is feasible within the proposed framework. The architecture follows a previously published OFS-to-Cloud IoT platform [49] by some of the authors, which details scalable MQTT communication and edge pre-processing. Raw FBG streams were acquired at 5 kHz (40 kB/s per sensor; 14 GB/day for four sensors) and locally pre-processed before transmission. For inference, signals were down-sampled to 17 Hz, normalized, and transmitted as sliding windows, significantly reducing bandwidth while preserving leak dynamics. The 45-window size (2.6 s) selected was used to define the detection latency; shorter windows were seen to reduce the robustness, while longer windows increased the delay. Cloud inference completed on a sub-second time scale, enabling near-real-time alarm generation.

Overall, XGBoost in the parallel mode emerged from the study as the most reliable and computationally efficient approach for FBG-based leak detection. This study is, to our knowledge, the first to compare systematically both supervised and unsupervised models using real-world FBG pressure data while assessing serial and parallel sensor configurations, providing practical deployment insights. Although limited to ≥7 mm leak events and imbalanced classes, this work has established a foundational step toward scalable ML-enabled FBG monitoring systems. Although the weighted precision and F1-scores appear modest, the results were obtained on a small, highly imbalanced real-world dataset using in situ FBG-based sensors. Benchmarking against three state-of-the-art models on the same data shows XGBoost achieved the highest precision (0.77), outperforming Spectral ANN (0.56), CNN–Bi LSTM (0.43), LS-SVM (0.31), and Naïve Bayes (0.29). As practical pipeline monitoring prioritizes precision (to minimize false alarms which can be very expensive), these results have established a realistic baseline for ML-driven FBG-based sensor systems, with further gains expected from larger datasets and use of multi-model fusion.

F. Comparative analysis

This section presents a comparative analysis to benchmark the proposed framework against highly cited ML-based leak detection studies [16], [21], [28]. The selected studies represent ML-based leak detection using pressure, vibration, or acoustic time-series data modalities closest to FBG-based sensing. It is important to emphasize that unlike most prior work based on simulated or laboratory data, this study used real FBG-based pressure measurements from a practical, large-scale, pipeline test facility. Few ML studies report real FBG-derived datasets, making these references a practical benchmark, while tackling successfully the challenges of real-world deployment. Sensor types, models, and results reported in the literature are summarized in Table IV.

TABLE IV
Comparative performance of benchmark ML models.

Study	Journal/ Year	Sensor Type	Model	Result
Yang [28]	AAAI Conf. Artificial Intelligence, 2021	Vibration and Acoustic DAS	CNN + Bi LSTM hybrid	97% accuracy
Zang [21]	Measurement, 2021	Electronic pressure sensors	LS-SVM, NB	98%, 95% accuracy
Islam [16]	IEEE Access, 2023	Acoustic	ANN	98% accuracy

This work has thus provided the first systematic ML-based evaluation using ‘real-world’ FBG pressure data. To enable a systematic comparison to be made, all benchmark models were re-implemented and evaluated using the same FBG-based dataset, with weighted comparative results shown in Table V.

TABLE V
Comparative performance of benchmark ML models.

Model	Weighted Average Precision	Weighted Average F1-Score
Naïve Bayes [21]	0.29	0.44
LS-SVM [21]	0.31	0.46
CNN +Bi LSTM [28]	0.43	0.41
SpectralANN [16]	0.56	0.58
XGBoost (This study)	0.77	0.52

The parallel XGBoost model (window = 45) achieved 0.77 precision, outperforming benchmark studies and showing robustness to noise and class imbalance in FBG-based data. Its F1-score (0.52) was slightly below the value of 0.58 reported by Islam et al. [16], likely because acoustic datasets exhibit sharper, more separable leak signatures than the gradual pressure responses induced in this study. Despite this, XGBoost has demonstrated a strong overall performance under more challenging conditions.

Confusion matrices of the re-implemented models (Fig. 13) further illustrate this differences. Zang et al.’s LS-SVM and Naïve Bayes models misclassified many no-leak points as

leaks, while Yang et al.'s CNN-Bi LSTM reduced false alarms but missed many leak points. Islam et al.'s ANN achieved a better balance but still underperformed compared to the precision achievable from XGBoost.

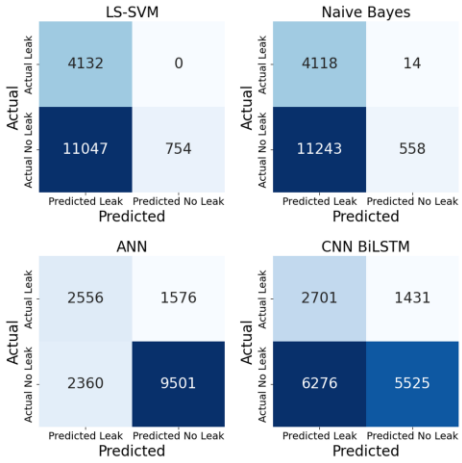

Fig. 13. Total confusion matrices for Zang et al.'s LS-SVM, Zang et al.'s Naïve Bayes, Islam et al.'s ANN, and Yang et al.'s CNN Bi LSTM.

V. Conclusion

This study undertaken has enabled a comparison of Random Forest, XGBoost, LSTM, and LSTM Autoencoder for pipeline leak detection using real-world FBG-based pressure data, under serial and parallel configurations, with varying window lengths. XGBoost achieved the best performance, reaching 77% precision in the parallel 45 window length, demonstrating that supervised tree-based models are more effective than unsupervised deep learning for small, imbalanced real-world datasets. Multi-sensor (parallel) training consistently outperformed single-sensor (serial) configurations, although serial deployment remains practical when underground access limits sensor availability.

Thus, the main contributions of this work can be summarized as:

1. A systematic comparison of supervised and unsupervised ML models trained on real-world, imbalanced FBG pressure sensor data for leak detection.
2. Successful evaluation of serial versus parallel sensor configurations and the effect of window length on model performance.
3. Benchmarking against three state-of-the-art approaches on the same dataset, confirming XGBoost as a robust choice for noisy, limited FBG pressure sensor data.

Future deployment of the approach can follow IoT-enabled architectures, such as our pervious implementation in [49], where FBG sourced data were transmitted from the interrogator to an edge device and then to the cloud via MQTT with lossless compression, enabling scalable real-time monitoring and alerting without changing the sensing methodology.

While the framework was seen to perform reliably for moderate and large leaks, the effective detection of very small leaks (<7 mm) remains more limited due to weak signal signatures and class imbalance, reflecting operation near the sensitivity limits of the sensing system. Future work will focus on larger, more balanced datasets across wider operating conditions and on multi-modal sensor fusion (e.g., combining FBG-based pressure with acoustic or temperature sensing) to improve robustness, particularly for early-stage and small-leak detection. Future work will integrate the models into the cloud platform for real-time anomaly detection and thus providing important alerts to the user, enabling a scalable FBG-based monitoring system that reduces environmental, financial, and public safety risks.

Acknowledgment

The authors gratefully acknowledge the support of Professors Simon Tait and Kirill V. Horoshenkov (University of Sheffield) for access to the National Distributed Water Infrastructure Facility. The first author also thanks City St George's, University of London for PhD scholarship support.

References

[1] M. Lillywhite and G. Stone, "Matson burst pipe: Residents 'flabbergasted' by 50ft jet of water," BBC News, May 14, 2025. Available: https://www.bbc.co.uk/news/articles/cd620lyqqnqo.

[2] "Oxford water main burst causes pressure issues," BBC News, Jul. 08, 2025. Available: https://www.bbc.co.uk/news/articles/cpd1ylevgdvo.

[3] Fabian, M., Scott, R., Bandyopadhyay, S., Sun, T., Grattan, K. T. V., Bustamante, H., . . . Hearfield, J. (2023). Novel Fibre Bragg Sensors to Quantify Pressure Transients in Pumping Stations. In 28th International Conference on Optical Fiber Sensors (pp. Tu3.92). Optica Publishing Group. Doi: 10.1364/ofs.2023.tu3.92.

[4] Rente, B., Fabian, M., Vidakovic, M., Vorreiter, L., Bustamante, H., Sun, T., & Grattan, K. T. V. (2021). Extended Study of Fiber Optic-Based Humidity Sensing System Performance for Sewer Network Condition Monitoring. IEEE Sensors Journal, 21(6), 7665-7671. doi:10.1109/jsen.2021.3050341.

[5] Rente, B., Fabian, M., Vidakovic, M., Sunarho, J., Bustamante, H., Sun, T., & Grattan, K. T. V. (2021). A Fiber Bragg Grating (FBG)-Based Sensor System for Anaerobic Biodigester Humidity Monitoring. IEEE Sensors Journal, 21(2), 1540-1547. doi:10.1109/jsen.2020.3017108.

[6] J. Zuo et al., "Pipeline Leak Detection Technology Based on Distributed Optical Fiber Acoustic Sensing System," IEEE Access, vol. 8, pp. 30789–30796, 2020, doi: https://doi.org/10.1109/access.2020.2973229.

[7] L. Wong et al., "Leak Detection in Water Pipes Using Submersible Optical Optic-Based Pressure Sensor," Sensors, vol. 18, no. 12, p. 4192, Nov. 2018, doi: https://doi.org/10.3390/s18124192.

[8] S. W. Jacobsz and S. I. Jahnke, "Leak detection on water pipelines in unsaturated ground by discrete fibre optic sensing," Structural Health Monitoring, vol. 19, no. 4, pp. 1219–1236, Oct. 2019, doi: https://doi.org/10.1177/1475921719881979.

[9] L.-X. Bian, J. Ma, C. Zhang, S.-K. Wang, F.-K. Shen, and H.-P. Wang, "Investigation on Sensor Layout of Optical Fiber Distributed Acoustic Sensing Technology for Flow Velocity Measurement in Pipes," IEEE Sensors Journal, vol. 24, no. 24, pp. 41814–41824, Dec. 2024, doi: https://doi.org/10.1109/jsen.2024.3481954.

[10] Z. Jia, L. Ren, H. Li, and W. Sun, "Pipeline Leak Localization Based on FBG Hoop Strain Sensors Combined with BP Neural Network," Applied Sciences, vol. 8, no. 2, pp. 146–146, Jan. 2018, Doi: https://doi.org/10.3390/app8020146.

[11] A. Venketeswaran et al., "Recent Advances in Machine Learning for Fiber Optic Sensor Applications," Advanced Intelligent Systems, vol. 4, no. 1, p. 2100067, Oct. 2021, Doi: https://doi.org/10.1002/aisy.202100067

[12] H Y. Zhou, Y. Zhang, Q. Yu, L. Ren, Q. Liu, and Y. Zhao, "Application of machine learning in optical fiber sensors," Measurement (London. Print), pp. 114391–114391, Feb. 2024, Doi: https://doi.org/10.1016/j.measurement.2024.114391.

[13] J. Alves Coelho, A. Glória, and P. Sebastião, "Precise Water Leak Detection Using Machine Learning and Real-Time Sensor Data," IoT, vol. 1, no. 2, pp. 474–493, Dec. 2020, Doi: https://doi.org/10.3390/iot1020026.

[14]Fahed Ebisi, I. P. Nikolakakos, Jayakumar Vandavasi Karunamurthi, A. Nasir, Eisa Al Buraimi, and Saeed Alblooshi, "Machine Learning Schemes for Leak Detection in IoT-enabled Water Transmission System," Mar. 2023, Doi: https://doi.org/10.1109/itikd56332.2023.10100175.

[15]Manel Boujelben, Zeineb Benmessaoud, M. Abid, and Manel Elleuchi, "An efficient system for water leak detection and localization based on IoT and lightweight deep learning," Internet of Things, vol. 24, pp. 100995–100995, Dec. 2023, Doi: https://doi.org/10.1016/j.iot.2023.100995.

[16]M. R. Islam, S. Azam, B. Shanmugam, and D. Mathur, "An Intelligent IoT and ML-Based Water Leakage Detection System," IEEE Access, vol. 11, pp. 123625–123649, 2023, Doi: https://doi.org/10.1109/ACCESS.2023.3329467.

[17]S. Ahmad, Z. Ahmad, C.-H. Kim, and J.-M. Kim, "A Method for Pipeline Leak Detection Based on Acoustic Imaging and Deep Learning," Sensors, vol.22, no. 4, p. 1562, Feb. 2022, Doi: https://doi.org/10.3390/s22041562.

[18]B. P. Duong, J. Kim, I. Jeong, C. H. Kim, and J.-M. Kim, "Acoustic Emission Burst Extraction for Multi-Level Leakage Detection in a Pipeline," Applied Sciences, vol. 10, no. 6, p. 1933, Mar. 2020, Doi: https://doi.org/10.3390/app10061933.

[19]G. Kousiopoulos, D. Kampelopoulos, N. Karagiorgos, G. Papastavrou, and S. Nikolaidis, "Acoustic Leak Localization Method for Pipelines in High-Noise Environment Using Time-Frequency Signal Segmentation," IEEE Transactions on Instrumentation and Measurement, vol. 71, p. 1, Jan. 2022, Doi: https://doi.org/10.1109/TIM.2022.3150864.

[20]N. Ullah, Z. Ahmed, and J.-M. Kim, "Pipeline Leakage Detection Using Acoustic Emission and Machine Learning Algorithms," Sensors, vol. 23, no. 6, p. 3226, Jan. 2023, Doi: https://doi.org/10.3390/s23063226.

[21]D. Zang, J. Liu, and F. Qu, "Pipeline small leak detection based on virtual sample generation and unified feature extraction," Measurement, vol. 184, p. 109960, Nov. 2021, Doi: https://doi.org/10.1016/j.measurement.2021.109960.

[22]J.-H. Kim, M. Chae, J.-S. Han, S. Park, and Y. Lee, "The development of leak detection model in subsea gas pipeline using machine learning," vol. 94, pp. 104134–104134, Oct. 2021, Doi: https://doi.org/10.1016/j.jngse.2021.104134.

[23]. M. Marin et al., "Assay of Metal Loss in Pipelines with Repaired Sleeves Using Machine-Learning-Assisted Fiber-Optic Distributed Acoustic Sensing," IEEE Sensors Journal, pp. 1–1, Jan. 2024, Doi: https://doi.org/10.1109/jsen.2024.3513433.

[24]X. Fan and X. (Bill) Yu, "An innovative machine learning based framework for water distribution network leakage detection and localization," Structural Health Monitoring, p. 147592172110402, Aug. 2021, Doi: https://doi.org/10.1177/14759217211040269.

[25]H. Yuan et al., "Real-time detection of urban gas pipeline leakage based on machine learning of IoT time-series data," Measurement, vol. 242, pp. 115937–115937, Oct. 2024, Doi: https://doi.org/10.1016/j.measurement.2024.115937.

[26]A. P. Ekong, G. G. James, and Ifeoma Ohaeri, "Oil and Gas Pipeline Leakage Detection using IoT and Deep Learning Algorithm," Journal of Information Systems and Informatics, vol. 6, no. 1, pp. 421–434, Mar. 2024, Doi: https://doi.org/10.51519/journalisi.v6i1.652.

[27]Y. Liu, X. Ma, Y. Li, Y. Tie, Y. Zhang, and J. Gao, "Water Pipeline Leakage Detection Based on Machine Learning and Wireless Sensor Networks," Sensors (Basel, Switzerland), vol. 19, no. 23, Nov. 2019, Doi: https://doi.org/10.3390/s19235086.

[28]Y. Yang, L. Yi, T. Zhang, Y. Zhou, and H. Zhang, "Early Safety Warnings for Long-Distance Pipelines: A Distributed Optical Fiber Sensor Machine Learning Approach," Proceedings of the ... AAAI Conference on Artificial Intelligence, vol. 35, no. 17, pp. 14991–14999, May 2021, Doi: https://doi.org/10.1609/aaai.v35i17.17759.

[29]H. Gemeinhardt and J. Sharma, "Machine-Learning-Assisted Leak Detection Using Distributed Temperature and Acoustic Sensors," IEEE Sensors Journal, vol. 24, no. 2, pp. 1520–1531, Dec. 2023, Doi: https://doi.org/10.1109/jsen.2023.3337284.

[30]A. Fares, I. A. Tijani, Z. Rui, and T. Zayed, "Leak detection in real water distribution networks based on acoustic emission and machine learning," Environmental Technology, pp. 1–17, May 2022, Doi: https://doi.org/10.1080/09593330.2022.2074320.

[31]Z. Peng et al., "Distributed fiber sensor and machine learning data analytics for pipeline protection against extrinsic intrusions and intrinsic corrosions," Optics Express, vol. 28, no. 19, pp. 27277–27277, Sep. 2020, Doi: https://doi.org/10.1364/oe.397509.

[32]Y. Liu, Y. Huang, and Y. Bao, "Machine learning-empowered automatic analysis of distributed fiber optic sensor data for monitoring coincident corrosion and cracks in pipelines," Measurement, pp. 116805–116805, Jan. 2025, Doi: https://doi.org/10.1016/j.measurement.2025.116805.

[33]U. Rajasekaran and Mohanaprasad Kothandaraman, "Comparative Analysis of Machine Learning and Deep Learning Based Water Pipeline Leak Detection Using EDFL Sensor," Journal of Pipeline Systems Engineering and Practice, vol. 14, no. 4, Nov. 2023, Doi: https://doi.org/10.1061/jpsea2.pseng-1439.

[34]L. Yang, Y. Guo, and S. Gao, "Multi-leak detection in pipeline based on optical fiber detection," Optik, vol. 220, p. 164996, Oct. 2020, Doi: https://doi.org/10.1016/j.ijleo.2020.164996.

[35]J. Zuo et al., "Pipeline Leak Detection Technology Based on Distributed Optical Fiber Acoustic Sensing System," IEEE Access, vol. 8, pp. 30789–30796, 2020, Doi: https://doi.org/10.1109/access.2020.2973229.

[36]Y. Zhou, Y. Zhang, Q. Yu, L. Ren, Q. Liu, and Y. Zhao, "Application of machine learning in optical fiber sensors," Measurement (London. Print), pp. 114391–114391, Feb. 2024, Doi: https://doi.org/10.1016/j.measurement.2024.114391.

[37]A. Venketeswaran, N. Lalam, J. Wuenschell, M. Buric, "Recent Advances in Machine Learning for Fiber Optic Sensor Applications," Advanced Intelligent Systems, vol. 4, no. 1, p. 2100067, Oct. 2021, Doi: https://doi.org/10.1002/aisy.202100067.

[38]M. Fabian, J. M Coote, R. Scott, T. Sun, K.T.V Grattan, H. Bustamante, T. Hillc, J. McCullochc, S. Taitd, K. Horoshenkov "Early leak detection in wastewater pipelines using fibre Bragg grating sensors," 26th International Conference on Optical Fiber Sensors, pp. 498–498, May 2025, doi: https://doi.org/10.1117/12.3062907.

[39]S. Han, B. D. Williamson, and Y. Fong, "Improving random forest predictions in small datasets from two-phase sampling designs," *BMC Medical Informatics and Decision Making*, vol. 21, p. 322, Nov. 2021, Doi: https://doi.org/10.1186/s12911-021-01688-3.

[40]C. Bentéjac, A. Csörgő, and G. Martínez-Muñoz, "A Comparative Analysis of Gradient Boosting Algorithms," Artificial Intelligence Review, vol. 54, no. 3, Aug. 2020, doi: https://doi.org/10.1007/s10462-020-09896-5.

[41]X. Yuan, L. Li, and Y. Wang, "Nonlinear Dynamic Soft Sensor Modeling with Supervised Long Short-Term Memory Network," IEEE Transactions on Industrial Informatics, vol. 16, no. 5, pp. 3168–3176, May 2020, Doi: https://doi.org/10.1109/tii.2019.2902129.

[42]Md. Nazmul Hasan, Sana Ullah Jan, and I. Koo, "Sensor Fault Detection and Classification Using Multi-Step-Ahead Prediction with an Long Short-Term Memory (LSTM) Autoencoder," Applied Sciences, vol. 14, no. 17, pp. 7717–7717, Sep. 2024, Doi: https://doi.org/10.3390/app14177717.

[43]J. Cheng and W. De Waele, "Weighted average algorithm: A novel meta-heuristic optimization algorithm based on the weighted average position concept," Knowledge-Based Systems, vol. 305, p. 112564, Dec. 2024, Doi: https://doi.org/10.1016/j.knosys.2024.112564.

[44]T.-S. Liou and M.-J. J. Wang, "Fuzzy weighted average: An improved algorithm," Fuzzy Sets and Systems, vol. 49, no. 3, pp. 307–315, Aug. 1992, Doi: https://doi.org/10.1016/0165-0114(92)90282-9.

[45]J. M. Merigó, "A unified model between the weighted average and the induced OWA operator," Expert Systems with Applications, vol. 38, no. 9, pp. 11560–11572, Sep. 2011, Doi: https://doi.org/10.1016/j.eswa.2011.03.034.

[46]N. Rogge, "Composite indicators as generalized benefit-of-the-doubt weighted averages," European Journal of Operational Research, vol. 267, no. 1, pp. 381–392, May 2018, Doi: https://doi.org/10.1016/j.ejor.2017.11.048.

[47]M. Mahesh, "The Essential Physics of Medical Imaging, Third Edition.," Medical Physics, vol. 40, no. 7, p. 077301, Jun. 2013, Doi: https://doi.org/10.1118/1.4811156.

[48]M. Welvaert and Y. Rosseel, "On the Definition of Signal-To-Noise Ratio and Contrast-To-Noise Ratio for fMRI Data," PLoS ONE, vol. 8, no. 11, p. e77089, Nov. 2013, Doi: https://doi.org/10.1371/journal.pone.0077089.

[49]H. Youssef, M. Fabian, T. Sun, M. Khanafer, H. Bustamante, and K. T. Grattan, "Work in Progress: Enhancing Sewage Systems Monitoring Through the Integration of Optical Fibre Sensors in IoT," pp. 574–576, Nov. 2024, Doi: https://doi.org/10.1109/wf-iot62078.2024.10811356.